Penetration of Cylindrical Objects in Soft Mud

Charles Aubeny, Texas A&M University
Department of Civil Engineering
College Station, TX 77843-3136

Wayne Dunlap, Texas A&M University
Department of Civil Engineering
College Station, TX 77843-3136

Abstract.- The depth of penetration of objects impacting into soft sediments in the seafloor will depend on a number of factors including sediment shear strength, impact velocity, orientation of the object, and the density of the object. A critical step in developing a model for predicting depth of penetration is establishing a database of impact penetration measurements under closely controlled conditions. Toward this end, researchers at Texas A&M University constructed a 4-ft deep by 6-foot diameter test basin for conducting impact tests. The penetration experiments used medium to high plasticity sediments collected from the Gulf of Mexico seafloor. Sediments were processed to achieve uniformity and shear strength characteristics were measured using miniature vane tests. Impact tests were conducted using an apparatus that could vary the object density, impact velocity and orientation. Test results were evaluated based on a simplified model that used plasticity theory to describe instantaneous soil resistance and a simple kinetic model to describe motions of the object. The test results indicated that sediment shear resistance is a critical factor controlling penetration depths.

I. INTRODUCTION

The depth of penetration of an object into soft seafloor sediments is relevant to a number of applications. Important examples include the performance of seafloor pipelines, “spudcan” foundations for jackup platforms, and waste disposal operations involving impact burial on the seafloor. In naval applications, predicting the depth of mine impact burial in cohesive sediments is a critical aspect of mine detection and clearing operations.

Researchers at Texas A&M University (TAMU) recently investigated this topic with single-gravity model tests of a cylinder penetrating into processed Gulf of Mexico sediments. The experimental data are interpreted within the framework of rate-dependent plasticity theory. This paper presents the results of preliminary interpretation of the test data.

II. ANALYTICAL FRAMEWORK

A simplified analytical framework developed for interpretation of the experimental data is presented below. Possible refinements to this model will be presented later in the paper. Fig. 1 shows the definition sketch for the analysis. The cylinder has a weight W, diameter d and length L, and the axis of the cylinder is assumed to have a horizontal orientation. At any given instant of time the bottom of the cylinder has penetrated a distance h into a soil having an undrained shearing resistance S_u and unit weight γ. The shearing resistance of the soil and buoyancy resist the weight of the cylinder.

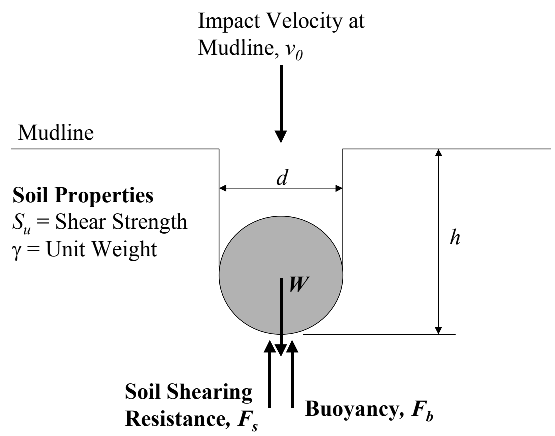

Figure 1. Definition Sketch

A. Equations of Motion

If the penetrating cylinder is modeled as a rigid particle, the instantaneous acceleration of the cylinder can be expressed in dimensionless form:

$$a/g = 1 - F_s / W - F_b / W \quad (1)$$

where a = acceleration of the cylinder
g = gravitational acceleration
F_s = soil shearing resistance force
F_b = buoyancy force

In cases where the soil bed is submerged, the buoyant weight W' of the cylinder should be used in Eq. 1.

Acceleration, velocity, penetration depth, and time may be expressed in dimensionless form as:

$$A = a / g \qquad (2a)$$

$$V = v / \sqrt{gd} \qquad (2b)$$

$$H = h / d \qquad (2c)$$

$$T = t\sqrt{d / g} \qquad (2d)$$

In which case, dimensionless velocity V and penetration H may be computed by integration of Eq. 1:

$$V = V_0 + \int A \, dT \qquad (3a)$$

$$H = \int V \, dT \qquad (3b)$$

As will be discussed subsequently, the resistance forces F_s and F_b are non-linear functions of penetration depth H. Hence, integration of Eqs. 3 must in general be performed numerically.

B. Soil Shearing Resistance

For the simplified analytical model developed in this research, the resisting force due to soil shear resistance, F_s, in Eq. 1 are estimated from plasticity theory [1]. The instantaneous soil resistance at any level of embedment h is estimated from a collapse load calculation. The effects of previous stresses and strains occurring in the soil earlier in the penetration process are neglected. For cylinders embedded less than one-half diameter (h/d < 0.5) in a purely cohesive soil of uniform strength, Murff et al. [2] present upper and lower bound solutions from plane strain plasticity theory. They show that, for h/d < 0.5, a reasonable approximation to their more rigorous plasticity solutions relates undrained shear strength S_u to the resisting force F_s by:

$$F_S = (S_u L \, d) 2 (2 + \pi) \sqrt{\frac{h}{d} - \left(\frac{h}{d}\right)^2} \qquad (4a)$$

The appropriate bearing factor for embedments that exceed one-half the cylinder diameter (h/d > 0.5) depend on how the soil flows around the top side of the penetrating cylinder. For the penetration tests conducted in this study, an open trench was observed to form above the cylinder when embedments greater than one-half the cylinder diameter occurred. Neglecting the contribution of shearing resistance in the soil above the center of the cylinder, the appropriate bearing factor is:

$$F_s = (S_u L \, d)(2 + \pi) \qquad h / d > 0.5 \qquad (4b)$$

C. Strain Rate Effects

The resisting forces F_s in Eqs. 4 are proportional to the undrained shear strength of the soil, which is actually a function of strain rate. In principle, a rate-dependent shear strength model can be incorporated into the plasticity formulation used to develop Eqs. 4. Research at TAMU is currently pursuing that possibility. As a simpler expedient, a strain rate correction can be applied directly to the F_s values in Eqs. 4. In this paper, a logarithmic strain rate correction is employed to get a corrected soil shear resistance force:

$$F_{sCOR} = F_s \left[1 + \lambda_{\text{cyl}} \; \log_{10} \left(\frac{v / \sqrt{gd}}{e_{ref} \; / \sqrt{g / d}} \right) \right] \qquad (5)$$

where e_{ref} is the reference strain rate measure corresponding to the undrained shear strength S_u, v is the instantaneous velocity of the penetrating cylinder, and λ_{cyl} is a multiplier. It is emphasized that λ_{cyl} is not an intrinsic material parameter since it is unique to the velocity and strain rate field of a penetrating cylinder. An empirical approach to selecting an appropriate strain rate multiplier will be discussed subsequently.

D. Buoyancy

A second component of resistance to penetration is the buoyancy of the soil displaced by the penetrating cylinder. The buoyant force can be calculated by multiplying the volume of the submerged portion of the cylinder by the unit weight of the soil. In addition, since an open trench forms above the cylinder, the trench volume must be added to the buoyancy calculation. The resistance to penetration from buoyancy can therefore be calculated from the following expression for h/d < 0.5:

$$F_b = (\gamma \; L d^2) \left[\frac{1}{4} \cos^{-1}\left(1 - \frac{2h}{d}\right) - \left(\frac{1}{2} - \frac{h}{d}\right) \sqrt{\frac{h}{d} - \left(\frac{h}{d}\right)^2} \right] \qquad (6a)$$

For penetration exceeding one-half diameter, h/d>0.5, the buoyant force becomes:

$$F_b = (\gamma \; L d^2) \left[\frac{\pi}{8} + \frac{h}{d} - \frac{1}{2} \right] \qquad (6b)$$

In cases where the soil bed is not submerged, such as in the model tests presented later in this paper, the total unit weight γ should be used in Eq. 6. Otherwise, the buoyant unit weight should be used.

D. Solutions

Solutions for Eq. 1 are conveniently expressed in terms of the following dimensionless parameters:

$$\text{Impact Velocity Ratio}: \; IVR = \frac{v_0}{\sqrt{gd}} \qquad (7a)$$

$$\text{Shear Resistance Ratio}: \; SRR = \frac{S_u L \, d}{W} \qquad (7b)$$

$$\text{Buoyancy Ratio}: \; BR = \frac{\gamma \, L \, d^2}{W} \qquad (7c)$$

Fig. 2 illustrates the relative influence of these variables. This figure plots predicted penetration for a constant

BR=0.5, with IVR varied from 0-3. The analyses used strain rate multiplier, λ_{cyl} = 0.10, with a reference strain rate measure, e = 0.02. As will be discussed subsequently, this reference strain rate measure corresponds to the standard rate of rotation in the vane shear tests used to measure the undrained shear strength, S_u. Fig. 2 clearly illustrates the strong influence of impact velocity v_0 and the soil shearing resistance S_u on penetration h/d.

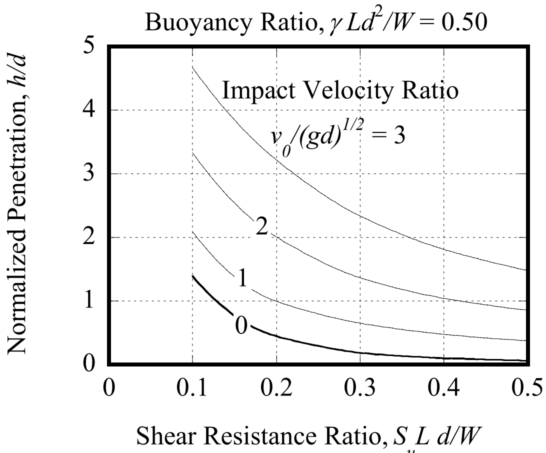

Figure 2. Predicted Effects of Impact Velocity and Soil Strength

III. EXPERIMENTAL PROGRAM

The experimental program [3] consisted of (1) sampling and processing the sediments to be used in the model experiments, (2) determining the relevant engineering properties of the sediments, (3) constructing a test basin and model cylinder, and (4) performing a series of penetration tests.

A. Sediment Preparation and Characterization

Sampling and Processing of Sediments.- Sediments for the experimental program were collected from the Gulf of Mexico seafloor approximately 20 miles south of Port Aransas. Offshore sampling was conducted on the research vessel *Longhorn* using a box core sampler. Thirty-five 55-gallon drums were filled with sediment and transported to Texas A&M University in College Station. The average moisture content of the collected sediments was about 69%. Atterberg limit tests showed the sediments to have liquid limits LL=44-45 and plastic limits PL=20-22. The sediments were processed to: (1) remove shells or other oversize materials that could adversely influence the model tests, (2) achieve uniformity with regard to material type and moisture content, and (3) achieve a uniform moisture content corresponding to an undrained shear strength of about 25 psf. Processing involved passing all material over a one-half inch screen, air drying the sediments from an initial moisture content of about 69% down to about 52%, and mixing by hand labor to achieve as high a degree of uniformity as practicable. Due to the tendency for a desiccation crust to form on the surface of the clay during air drying, the sediment had to be re-mixed on essentially a daily basis. The rate of drying of the sediments largely controlled the overall timetable for processing of the sediments, which required about 8 weeks to produce the required volume for the experimental model tests.

After processing, the sediments were tested at random locations for moisture content, hand vane shear strength, and percent fines (percent passing the #200 sieve). The test data are summarized in Table 1. The relationship between moisture content and hand vane shear strength is shown in Fig. 3. The data show considerable scatter; nevertheless, extension of the trend line of the moisture-strength down to the liquid limit (44-45) indicates an undrained shear strength at the liquid limit S_{uLL} = 50psf, which is in accord with Casagrande's estimate of soil strength at the liquid limit [4]. It should be noted that additional mixing occurred when the processed sediments were placed in the test basin. The hand vane tests were performed approximately 24 hours after any mixing operations.

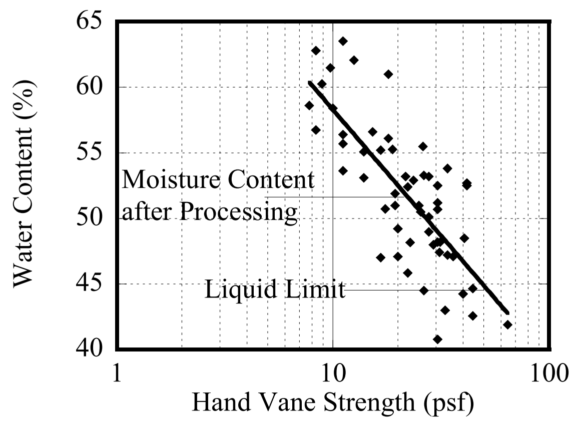

Figure 3. Strength vs. Water Content for Clay Used in Tests

As noted earlier, the undrained shear S_u strength of clay sediments is typically rate-dependent. To assess this effect for the clay used in these experiments miniature vane shear tests were conducted at variable rotation rates. The standard rotation rate for this test is 0.02 rad/sec. One miniature vane test was performed at 0.026 rad/sec, approximately the standard rotation rate. Additional tests were performed at 0.0013, 0.012, and 0.205 rad/sec. Measured torque corresponding to these rotation rates is plotted in Fig. 4. The data indicate that the maximum resisting torque increases by about 10 percent for each log cycle increase in rotation rate.

B. Experimental Apparatus

Basic components of the experimental apparatus included the following:

- *Test basin.* A 6-ft diameter by 4-ft deep galvanized steel tank comprises the test basin.

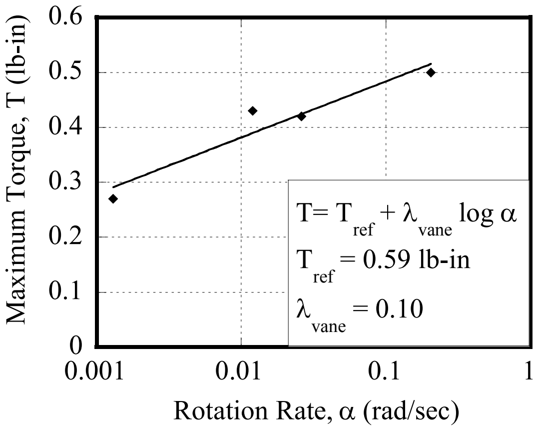

Figure 4. Variable Rotation Rate Vane Shear Tests

• *Test cylinder*. The model cylinder is comprised of a 6.625-inch diameter by 19.875-inch long hollow aluminum cylinder with hemispherical ends (Fig. 5). A guide rod is attached to the top of the cylinder to maintain the alignment and orientation of the cylinder as it penetrated into the sediment. The attachment angle between the guide rod and the cylinder can be adjusted to between 0 and 22°. A flat steel plate is attached to the top of the guide rod. Weights were placed on the steel plate to allow penetration tests for various cylinder weights. The minimum weight that could be tested was the weight of the cylinder, guide shaft, and plate – a total of 36.63 lb.

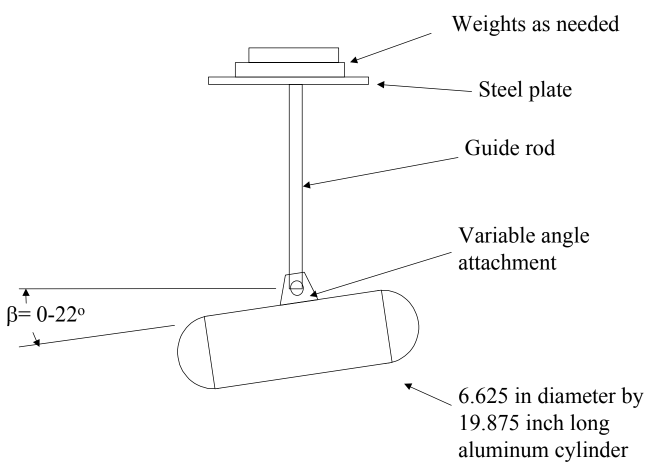

Figure 5. Model Penetrating Cylinder (not to scale)

• *Mine drop apparatus*. Mounted on top of the tank is the apparatus designed to facilitate the mine drops (Fig. 6). The apparatus is comprised of an approximately 6-ft diameter ring with a planar steel frame spanning the diameter of the ring. The circular ring was fabricated from 2-inch steel angle section and can be manually rotated when smoothing the surface of the sediment, as will be discussed subsequently. The planar steel frame was fabricated from 2-inch square tubing and welded to the circular ring. Two circular steel guide sleeves are welded to the planar frame. These sleeves serve as guides for mounting a steel screed apparatus for smoothing the surface of the sediment. The screed apparatus is comprised of steel plate attached to steel bars that fit through the guide sleeves on the planar frame. Prior to smoothing the sediment, the screed apparatus is lowered through the guides on the planar frame such that the steel screed plate is at the level of the sediment. By manually rotating the 6-ft diameter circular ring, the screed is dragged along the surface of the sediment to create a smooth, level surface. Two linear ball bushings mounted on the planar maintain the guide rod in a vertical position during penetration testing. The sediment tank was centered beneath a winch mounted to the ceiling of the laboratory in which the tests were performed. The winch was used to raise the cylinder to the desired elevation for each drop test.

• *Penetration measurements*. Mine penetration is measured by measuring the relative displacement between the steel plate on top of the guide rod (Fig. 2) and the planar frame (Fig. 6). In the original series of tests, involving cylinder penetration for the case of the cylinder initially resting on the surface of the sediment, penetration was measured manually. For subsequent drop tests, the relative location between the planar frame and the steel plate was measured with a magnetic linear displacement transducer.

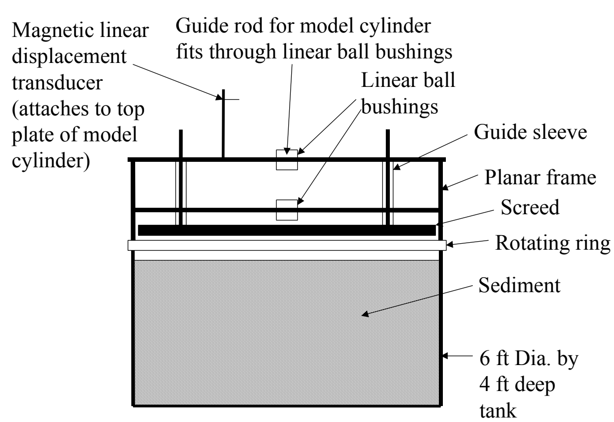

Figure 6. Test Basin Schematic (not to scale)

C. Test Procedure

Each test was performed as follows:

1. The sediment was mixed and remolded using a motorized stirrer. The sediment was allowed to set for approximately 24 hours after stirring.
2. The sediment surface was smoothed by rotating the screed shown in Fig. 3.
3. The cylinder was rotated to the desired orientation from horizontal. The bolt connecting the model cylinder to the guide rod was securely tightened to ensure a constant cylinder orientation during penetration.
4. The desired weight was loaded onto the steel plate on top of the guide rod.

5. The model cylinder was hoisted by a winch to the desired drop elevation.
6. The model cylinder was released and penetration versus time measurements were made for a time period of up to 24 hours.
7. Shear strength was measured at 4 to 5 locations around the cylinder with a hand vane. The strength was measured at approximately 6 inches beneath the sediment surface.

D. Test Program

The test program was conducted to investigate the effects of cylinder weight, impact velocity, cylinder orientation, and pre-embedment on penetration. The following discussion will focus on the first two variables: cylinder weight, W, and impact velocity, v_0. The test program was sub-divided into two series of tests. The first series involved non-impact tests in which the bottom of the cylinder was set at the elevation of the mudline prior to release, i.e., $v_0 = 0$. The second series involved impact tests in which the cylinder was dropped from a height of about 7 inches above the mudline, with impact velocities v_0 ranging from 5.8 to 6.79 ft/sec. Test results are summarized in Tables 1 and 2.

TABLE 1
Summary of Non-Impact Tests

Test No.	W (lbs)	S_u (psf)	h (in) after 1 min	H (in) 128 min
1	36.63	28.5	0.55	0.69*
5	102.63	25.5	2.74	3.70
7	124.63	21.8	4.42	5.74
8	142.23	28.0	4.25	6.02
9	168.63	29.9	6.10	8.77

*Measurement taken after 60 min.

TABLE 2
Summary of Impact Tests

Test No.	W (lbs)	S_u (psf)	v_0 (in/sec)	h (in) 1 sec	h (in) 24 hrs
22	63.03	38.9	7.06	4.67	4.84
23	102.63	25.0	7.07	8.43	8.67
24	168.63	41.3	7.56	9.29	10.02
25[1]	63.03	29.2	6.08	4.58	4.87
26[1]	102.63	29.1	6.46	8.23	8.48
27[1]	168.63	33.3	7.32	12.62	13.06
28[2]	63.03	25.0	6.95	8.66	8.82
29[2]	102.63	30.6	5.78	8.63	8.95
39[2]	168.63	30.9	5.25	13.72	14.42

1 - Cylinder oriented 10 degrees from horizontal.
2 - Cylinder oriented 20 degrees from horizontal.

One of the major observed differences between the non-impact and impact tests was that, for the non-impact tests, after initial penetration the cylinder continued to penetrate into the sediment for a time period of 24 hrs and beyond. A typical example of this time-dependent penetration is shown in Fig. 7. This additional penetration was quite significant, on the order of 50% of the initial penetration (Table 1). Likely causes of this additional penetration could be consolidation and/or creep. In the impact tests, the measured additional penetration following the initial impact penetration was quite small, typically on the order of 5% after 24 hours (Table 2).

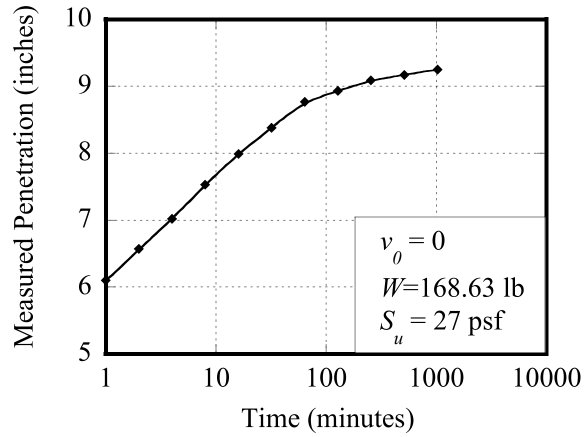

Figure 7. Typical Time-Dependent Penetration

Two visual observations of significance should also be noted with regard to the model tests. The first is that when the penetration exceeds one-half the cylinder diameter, $h/d > 0.5$, an open trench forms above the cylinder. This effect is quite significant in the development of Eqs. 4 and 6 presented earlier, which compute the soil shear resistance force F_s and the buoyancy force F_b. The second observation is that significant crack patterns formed around the penetrating cylinder. Hence, any models based on a continuum formulation may have to be considered qualitative in nature.

IV. EVALUATION OF TEST DATA

The experimental measurements obtained from the above test program were compared to predictions from the simple analytical model presented earlier. Strength, cylinder weight, and impact velocity inputs into the model (S_u, W, v_0) for each test are shown in Tables 1 and 2. A total unit weight of sediment $\gamma = 106$ pcf was used in the computation of the buoyancy ratio (Eq. 7c) for all predictions. The reference strain rate measure was taken as e =0.02, the standard strain rate for the miniature and hand vane tests that were used to estimate the shear strength S_u. Predictions were made for values of the strain rate multiplier (Eq. 5) varying between λ_{cyl} = 0 to 0.10. Comparisons between measurements and predictions are presented below.

Fig. 8 presents comparisons of predicted versus measured cylinder penetration based on the non-impact test data shown in Table 1. The comparisons indicate that if no correction is made for strain rate effects (λ_{cyl} = 0) the predicted penetrations over-estimate the measured values by about 50%. Predicted penetrations based on a strain rate multiplier λ_{cyl} = 0.10 are in close agreement with measurements. It is interesting to note that the strain rate multiplier that achieves optimal agreement between predicted and measured penetrations in the cylinder penetration tests match the strain rate multiplier relating torque to rotation rate in miniature vane tests λ_{vane} (Fig. 4).

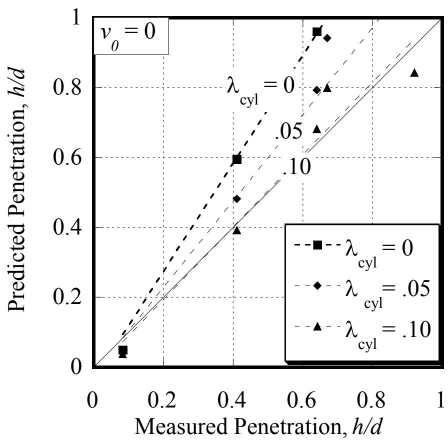

Figure 8. Prediction vs. Measurement for Non-Impact Tests

This match is to a considerable extent fortuitous, since λ_{cyl} and λ_{vane} correspond to different deformation fields. Nevertheless, this fortuitous match introduces the possibility that the strain rate multiplier obtained from variable rotation rate vane shear tests can provide a reasonable estimate of λ_{cyl} for penetration calculations.

Fig. 9 presents comparisons between predicted and measured penetrations for the impact tests summarized in Table 2. As was the case for the non-impact tests, predictions made assuming no strain rate effects ($\lambda_{cyl} = 0$) tend to over-predict actual penetrations. Assumption of a strain rate multiplier $\lambda_{cyl} = 0.10$ produces optimal matching between predictions and measurements.

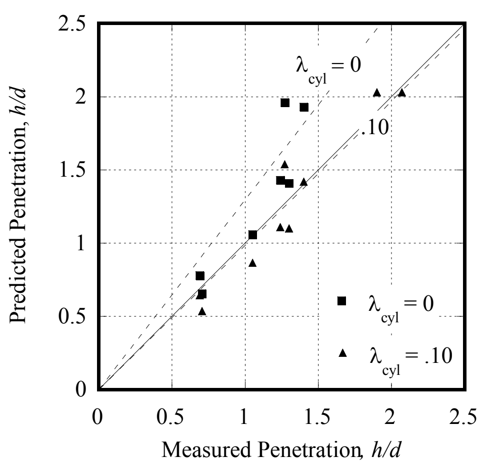

Figure 9. Prediction vs. Measurement for Impact Tests

V. CONCLUSIONS

Interpretation of model test data for cylindrical objects penetrating into soft sediments and development of an analytical model to characterize this process are still in progress at TAMU. Tentative conclusions from the experimental and analytical study are as follows:

1. Visual observations from the tests indicate that an open trench forms above the penetrating cylinder. Any analytical model formulations that are developed for predicting penetration should be consistent with this observation.
2. The penetration process for the non-impact case ($v_0 = 0$) appears to be a two-stage process: an initial penetration followed by time-dependent penetration that is probably associated with consolidation. The magnitude of this time-dependent penetration is at least one-half of the initial penetration; hence, this time-dependent penetration cannot be reasonably neglected.
3. Time-dependent penetration also occurs for impacting cylinders (v_0 around 6 fps), but its magnitude relative to the initial penetration is relatively small, typically on the order of 5%.
4. Plastic limit analyses appear to provide a suitable framework for developing a simplified predictive model for cylinders penetrating into soft seafloor sediments.
5. The strain rate dependence of the sediment shearing resistance appears to be of considerable significance. The use of shear strength estimates based on the relatively low strain rates associated conventional shear strength tests can result in under-estimates of the actual shearing resistance and over-estimates of penetration by about 50%.
6. Vane tests performed at variable rotation rates can provide reasonable estimates of the strain rate dependence of the shearing resistance of the sediments.

Acknowledgements

The authors would like to acknowledge the support of the Department of Defense Office of Naval Research. The authors would also like to acknowledge the guidance from Phil Valent and Andrei Abilev from the Naval Research Laboratory.

References

[1] Chen, W.F., *Limit Analysis and Plasticity*, Rotterdam: Elsevier, 1975.

[2] Murff, J.D., Wagner, D.A., and Randolph, M.F. "Pipe penetration in cohesive soil," *Geotechnique* 39, No. 2, pp.213-229, 1989.

[3] Munim, M.S., *An Experimental Investigation of Mine Burial Penetration in Soft Sediments*, Master of Science report, College Station, TX: Texas A&M University, 2003.

[4] Das, B.M. *Principles of Geotechnical Engineering 4^{th} Edition*, Boston: PWS Publishing Company, 1998.